ELSEVIER

Journal of Alloys and Compounds 281 (1998) 275–279

Journal of ALLOYS AND COMPOUNDS

Structure of $Al_{50}Ti_{50-x}Fe_x$ alloys prepared by mechanical alloying and subsequent annealing

A.V. Leonov[a,*], V.I. Fadeeva[a], O.E. Gladilina[a], H. Matyja[b]

[a]*Dept. of Chemistry, Moscow State University Leninski Gory, 119899, Moscow, Russia*
[b]*Dept. of Materials Science and Engineering, Warsaw University of Technology, Narbutta 85, 02-524 Warsaw, Poland*

Received 27 May 1998; received in revised form 30 June 1998

Abstract

The influence of ball milling in a high energy planetary mill on the phase formation in $Al_{50}Ti_{50-x}Fe_x$ (x=10, 20, 30, 40 at.%) powder mixtures was studied by X-ray diffraction (XRD) and differential scanning calorimetry (DSC). Mechanical alloying (MA) leads to the formation of single phase nanocrystalline alloys. Their structures depend on the initial composition of powder mixtures: hcp(C14), x=10; fcc(D8a), x=20, 30; bcc(B2), x=40. The MA alloys preserve their nanocrystalline state in the course of heating up to 500°C.

Keywords: Mechanical alloying; Al–Ti–Fe alloys; Structure

1. Introduction

Alloys based on aluminium intermetallics have potential as materials for use at high temperature applications. However, wide application of such materials is hampered by brittleness of the intermetallic phases. One of the ways towards highly ductile species consists in decreasing the grain size of the intermetallics [1]. From this point of view, formation of nanostructural materials is of particular interest. Mechanical alloying (MA) allows the formation of nanocrystalline structure for a large number of alloys [2–4]. Recently much attention has been given to investigations of metastable phases in the systems Al–Ti and Al–Fe produced by MA. The formation of different phases was reported in the binary system Al–Ti for the composition $Al_{50}Ti_{50}$: a hexagonal phase α_2 [5], an amorphous alloy [5–7] or a supersaturated solid solution Ti(Al) [8,13]. It was noted that in the system Al–Fe at the equiatomic composition $Al_{50}Fe_{50}$ a bcc solid solution Fe(Al) formed in most of the cases [9,10].

Another possibility for increasing ductility of aluminium based alloys is the additional alloying with transition metals that leads to the formation of complex intermetallics. The most interesting phases are those which have high symmetry, for example cubic. The presence of a ductile cubic phase allows an increasing ductility of the whole alloy [11]. In this respect the system Al–Ti–Fe has good potential. In accordance with the Al–Ti–Fe phase diagram [12] (Fig. 1), there are binary intermetallics of high practical importance. In addition, ternary intermetallics, with cubic structure can be seen. One of the latter, the τ_3 phase ($Al_{22}Fe_3Ti_8$), has a cubic $L1_2$ structure type. Other ternary intermetallic (τ_2 or Al_2FeTi) have an fcc structure

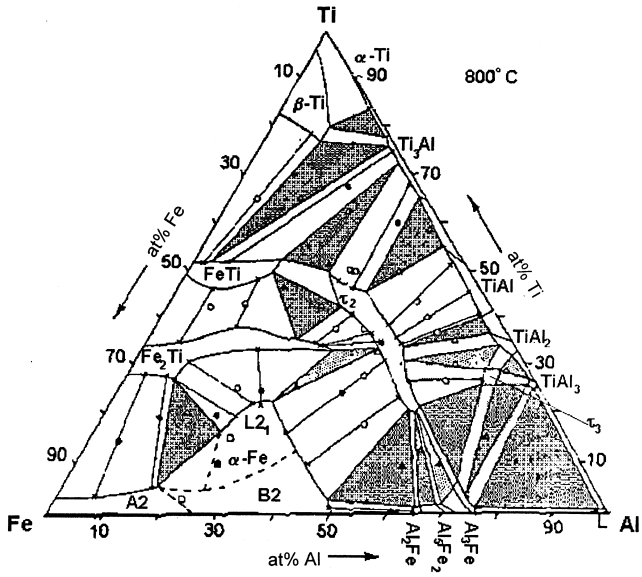

Fig. 1. Isothermal section of the Fe–Al–Ti system at 800°C [[12]].

*Corresponding author. E-mail: leonov@general.chem.msu.ru

0925-8388/98/$ – see front matter
PII: S0925-8388(98)00730-0

of the type D8a. Furthermore, it was shown [12], that phase τ_2 is cubic when the Ti content is high, and tetragonal, when the Ti content is low.

Here we report the investigation of structure and phase transformations during mechanical alloying of ternary $Al_{50}Ti_{50-x}Fe_x$ including the stability of the formed phases under thermal annealing.

2. Experimental details

Mixtures of powders of pure metals with the compositions $Al_{50}Ti_{50-x}Fe_x$ (where $x=10$, 20, 30, 40 at%) were prepared. We used metal powders with purities not lower than 99.7%. The particle sizes were not larger than 40, 250 and 100 μm for Al, Ti and Fe, respectively. Mechanical alloying was performed in a high energy planetary ball mill with stainless steel vials and balls with diameters of 7.8 mm under an Ar atmosphere. Vials were cooled with water in the course of milling. Milling was performed in a milling-pause regime (5 min milling followed by 10–15 min pause) for better cooling of the system. The mass of the powder mixture loaded into one vial was 5 g. In our experiments the ball to powder mass ratio was 9:1. The milling process was interrupted at desired milling times and a small amount of powder was taken out of the vials for analysis. The MA samples were examined by using X-ray diffraction (XDR) and differential scanning calorimetry (DSC). XDR analysis was performed on a DRON-4 X- ray powder diffractometer with a graphite monochromator and CuKα radiation. Thermal analysis of the mechanically alloyed powders was carried out up to 700°C using a Perkin- Elmer DSC-7 at a heating rate of 20°C min^{-1} in an Ar atmosphere. A Perkin-Elmer DSC-7 has also been used to perform the thermal treatments up to 700°C. Continuous thermal annealing over 2 h at 800°C was carried out in evacuated quartz ampoules.

The chemical compositions of the MA alloys were checked by a microanalyser of type 'Camebax-Mikrobeam' with powders pressed into tablets.

3. Results and discussion

X-ray diffraction pattern of all powder mixtures after MA for 2 h did not show reflections of the initial components (Fig. 2). The phase composition of the samples did not change when the milling time was increased. Thus, the solid phase interaction between the initial components were completed, and structures which were stable under these conditions of MA were formed.

The chemical composition of the powders after mechanical alloying is shown in Table 1. Deviations of the composition of the MA alloys from the composition of the initial powder mixtures could be due to partial adherence

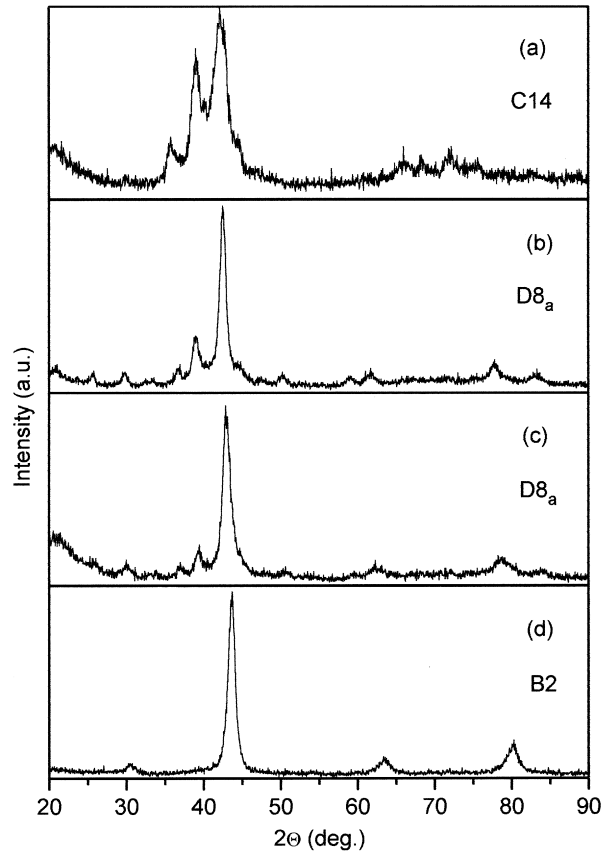

Fig. 2. XDR patterns of $Al_{50}Ti_{50-x}Fe_x$ alloys after 2 h of MA: (a) $x=10$, (b) $x=20$, (c) $x=30$, (d) $x=40$.

of Al to the balls and walls of the vial and to possible contamination by the material of the milling tools.

During mechanical alloying of the powders, the $Al_{50}Ti_{40}Fe_{10}$ phase with hcp structure type C14 and lattice parameters $a=0.503$ nm, $c=0.820$ nm was formed (Fig. 2a). A similar structure is observed for the Fe_2Ti phase in which a considerable quantity of Al can be dissolved (Fig. 1). It was shown [12], that solubility of Al in Fe_2Ti increase from 33.5% to 47.0 at.% when the temperature was increased from 800 to 1000°C. Thus one can suppose the formation of a metastable phase with C14 structure by MA.

Milling of powder mixtures of the composition $Al_{50}Ti_{30}Fe_{20}$ leads to the formation of a single-phase alloy with fcc structure of type D8a with the lattice parameter $a=1.2050$ nm (Fig. 2b). The same cubic structure (D8a)

Table 1
Chemical composition of mechanically alloyed Al–Ti–Fe alloys (in atomic percent)

Sample	Al	Ti	Fe
$Al_{50}Ti_{40}Fe_{10}$	48.5	39.3	12.2
$Al_{50}Ti_{30}Fe_{20}$	49.7	29.8	20.5
$Al_{50}Ti_{20}Fe_{30}$	50.2	19.5	30.3
$Al_{50}Ti_{10}Fe_{40}$	47.5	10.1	42.4

was also formed by MA of mixtures containing 30 at.% Fe. However, in this case the X-ray patterns (Fig. 2c) reveal changes in intensity of several lines as compared to that of the alloy $Al_{50}Ti_{30}Fe_{20}$ and the lattice parameter of the fcc phase for the $Al_{50}Ti_{20}Fe_{30}$ alloy is lower (a=1.191 nm). The X-ray diffraction pattern of $Al_{50}Ti_{10}Fe_{40}$ powders registered after mechanical treatment of these powders indicates the formation of a cubic phase with B2 structure. Thus, decreasing the titanium content in MA alloys corresponding to the quasibinary section $Al_{50}Ti_{50}$–$Al_{50}lFe_{50}$ is accompanied by a transition of the hexagonal structure to a cubic one.

It has been shown in Refs. [8,13], that a supersaturated solid solution α-Ti(Al) with hcp structure of type A3 was formed by MA of equiatomic $Al_{50}Ti_{50}$ mixtures. Partial replacement of Ti by 10 at.% Fe results in the hexagonal phase (β_{ss}) with C14 structure type.

For MA $Al_{50}Fe_{50}$ powders, the formation of a bcc phase (A2 structure) was observed [9,10]. In the Fe-rich region, replacement of Fe by 10 at.% Ti leads to the formation of the α_{ss} phase with ordered B2 structure in the course of milling. At the same time, in the two- component Al-Fe system annealing is needed to form the ordered phase AlFe [10]. According to the phase diagram (Fig. 1), the solubility of Ti in the AlFe compound is not more than 3 at.% Ti at 800°C. Mechanical alloying results in a considerable broadening of the region where the ordered B2 structure exists.

According to the phase diagram (Fig. 1), the $Al_{50}Ti_{30}Fe_{20}$ alloy is close to the region of the τ_2 phase which is characterized by a wide homogeneity range. MA of a powder mixture of this composition leads to the formation of τ_2 with cubic structure (D8a).

The $Al_{50}Ti_{20}Fe_{30}$ alloy is two-phase ($\tau_2+\alpha_{ss}$) in its equilibrium state. It was noted above, that the structure of MA $Al_{50}Ti_{20}Fe_{30}$ and $Al_{50}Ti_{30}Fe_{20}$ alloys are similar and can be described as fcc (D8a). However, in the $Al_{50}Ti_{20}Fe_{30}$ alloy it is possible to distinguish the B2 structure with a lattice parameter a=0.297 nm when the intensity of the X-ray diffraction lines of $Al_{50}Ti_{30}Fe_{20}$ and $Al_{50}Ti_{20}Fe_{30}$ (Fig. 2b,c) are compared. In the latter case one should observe a superposition of X-ray lines such as $(400)\tau_2+(100)\alpha_{ss}$, $(440)\tau_2+(110)\ \alpha_{ss}$, and so on. It is possible that these phases become coherent. Hence, we can characterize the MA $Al_{50}Ti_{20}Fe_{30}$ alloy either as one-phase τ_2 with cubic structure (D8a), or as two-phase ($\tau_2+\alpha_{ss}$). In the latter case the ratio of lattice parameters $a(\tau_2)$: $a(\alpha_{ss})$ must be 4:1.

The influence of high temperature annealing on the structure and phase composition of MA powders was studied by heating specimens for 2 h at 800°C in vacuum. In Table 2 the characteristics of structures that are formed as a result of mechanical alloying and high temperature annealing are summarised.

X-ray patterns of annealed specimens at 800°C are shown in Fig. 3. Two phases are formed in the $Al_{50}Ti_{40}Fe_{10}$ alloy. These phases are AlTi (L1o) and τ_2 (D8a) as seen in Fig. 3a. They corresponded to the equilibrium phases for this alloy composition [12].

The single-phase state of $Al_{50}Ti_{30}Fe_{20}$ alloy did not change in the course of heating at 800°C. At the same time, a decreasing diffraction peak width is observed. An increasing in the crystallite size and removal of the structural defects could explain this effect. The structure of the τ_2 phase is also preserved as a cubic (Fig. 3b). Annealed alloys containing 30 and 40 at.% Fe are two-phase with different contents of the τ_2 and α_{ss} phases (Fig. 3c,d). Thus, high temperature annealing of the MA $Al_{50}Ti_{50-x}Fe_x$ alloys at 800°C leads to states which are in good agreement with the phase diagram shown in Fig. 1.

The transformations from the metastable state to the equilibrium state were studied by using DSC and XRD. In Fig. 4 are shown the DSC curves after subtracting the data obtained after second heating. For the $Al_{50}Ti_{40}Fe_{10}$ and $Al_{50}Ti_{30}Fe_{20}$ alloys, endothermic effects are observed. Exothermic effects appear for alloys with lower Ti content. The desorption of the gas contamination might be a possible reason for the endothermic effects in the DSC

Table 2
Phase and structure characteristics of $Al_{50}Ti_{50-x}Fe_x$ alloys after MA and annealing at 800°C

Sample	MA			Annealing		
	Phase	Structure type	Lattice parameters, nm	Phase	Structure type	Lattice parameters nm
Al_50_{Ti50} [13]	Ti(Al)	A3	a=0.2865(5) c=0.4605(5)	AlTi	L1o	a=0.3992(1) c=0.4072(2)
$Al_{50}Ti_{40}Fe_{10}$	β_{ss}	C14	a=0.503(2) c=0.820(2)	Al(Ti,Fe)	L1o	a=0.3992(1) c=0.4077(2)
				τ_2	D8a	a=1.2061(2)
$Al_{50}Ti_{30}Fe_{20}$	τ_2	D8a	a=1.2050(5)	τ_2	D8a	a=1.2036(2)
$Al_{50}Ti_{20}Fe_{30}$	τ_2	D8a	a=1.191(1)	τ_2	D8a	a=1.1953(3)
				Al(Fe,Ti)	B2	a=0.2928(2)
$Al_{50}Ti_{10}Fe_{40}$	α_{ss}	B2	a=0.2935(3)	Al(Fe,Ti)	B2	a=0.2919(1)
				τ_2	D8a	a=1.1925(4)
$Al_{50}Fe_{50}$ [10]	Fe(Al)	A2	a=0.2909(3)	AlFe	B2	a=0.2901(2)

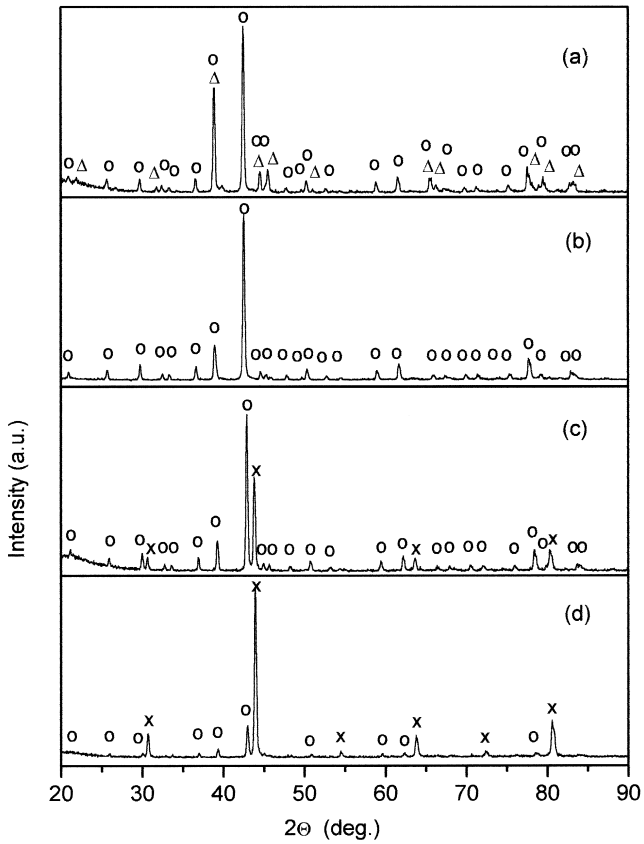

Fig. 3. XDR patterns of mechanical alloyed $Al_{50}Ti_{50-x}Fe_x$ alloys after annealing at 800°C, 2 h: (a) $x=10$; (b) $x=20$; (c) $x=30$; (d) $x=40$ at.% Fe, ○-τ_2 (D8a); △-Al(Ti, Fe) (L1o); ×-Al(Fe, Ti) (B2).

curves, since the alloys with higher Ti content reveal greater absorption capability.

It was found [13], that the powders of the $Al_{50}Ti_{50}$ alloy obtained by ball milling under argon atmosphere contained absorbed hydrogen. According to the thermodesorption results, release of hydrogen occurs within the temperature range 400°C–600°C. This is the temperature range where the endothermic effects in the DSC curves are observed (Fig. 4a,b). Their magnitude may depend on the quantity of hydrogen in the specimens.

Thus, one can consider the DSC curves as a superposition of exothermic effects (the transformation of metastable phases to equilibrium) and endothermic effects (the desorption of gas contamination).

The phase composition of MA $Al_{50}Ti_{50-x}Fe_x$ alloys does not change in the course of heating up to 500°C. Further heating to 600–700°C leads to the formation of phases similar to those obtained after isothermal annealing at 800°C (Table 2).

The sequence of structural changes was investigated during heating of single-phase MA $Al_{50}Ti_{30}Fe_{20}$ and $Al_{50}Ti_{10}Fe_{40}$ alloys consisting of τ_2 and α_{ss} phases, respectively. In Fig. 5 the changes in the lattice parameters and the crystallite size as a function of annealing temperature are shown. Values of the crystallite size and microstrains were obtained by an approximation method, using the (400) and (800) X-ray lines for the D8a structure and the (110) and (211) lines for the B2 structure. The use

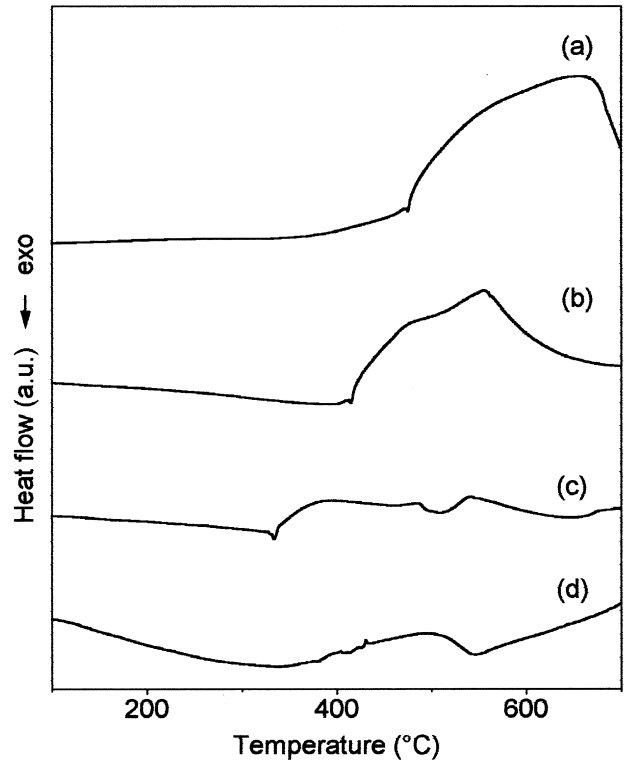

Fig. 4. DSC curves of mechanical alloyed $Al_{50}Ti_{50-x}Fe_x$ alloys: (a) $x=10$; (b) $x=20$; (c) $x=30$; (d) $x=40$ at.% Fe.

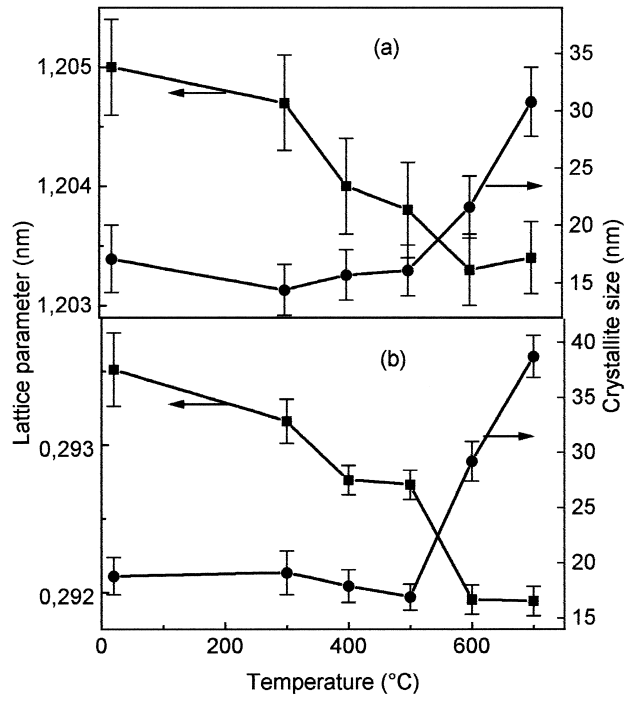

Fig. 5. Evolution vs. annealing temperature of the lattice parameter (■) and crystallite size (●) of $Al_{50}Ti_{30}Fe_{20}$ (a) and $Al_{50}Ti_{10}Fe_{40}$ (b) alloys.

of the (211) line instead of the (220) line is appropriate, since the Young-moduli coincide for these directions. A Lorentz function was chosen for this approximation. The powders annealed at 800°C for 2 h were used as a standard.

It is obvious (Fig. 5) that the crystallite sizes of the τ_2 and α_{ss} phases change slightly as a result of heating up to 500°C and increase with further increasing temperature. The lattice parameter of the τ_2 phase (Fig. 5a) does not change up to 300°C, but decreases in the temperature range of 300–600°C. The decrease of the lattice parameter of the τ_2 phase may be due to chemical ordering as well as to a release of absorbed gases, since no phase changes occur in the $Al_{50}Ti_{30}Fe_{20}$ alloy during heating. The decreasing lattice parameter of the α_{ss} phase in the $Al_{50}Ti_{10}Fe_{40}$ alloy (Fig. 5b) is in a good agreement with the DSC results (Fig. 4d), where two exothermic effects are observed. The low-temperature exothermic effect at 100–500°C is connected with removal of defects and with increasing long-range order. The latter follows from the increasing intensity ratio of the (100) superlattice line (I_{100}) to the (110) fundamental line (I_{110}) as shown in (Fig. 6). The second exothermic effect in the temperature range of 500–600°C leads to a further decrease of the lattice parameter of the α_{ss} phase and the formation of the cubic τ_2 phase. Simultaneously, long-range order of the α_{ss} phase is increasing (Fig. 6).

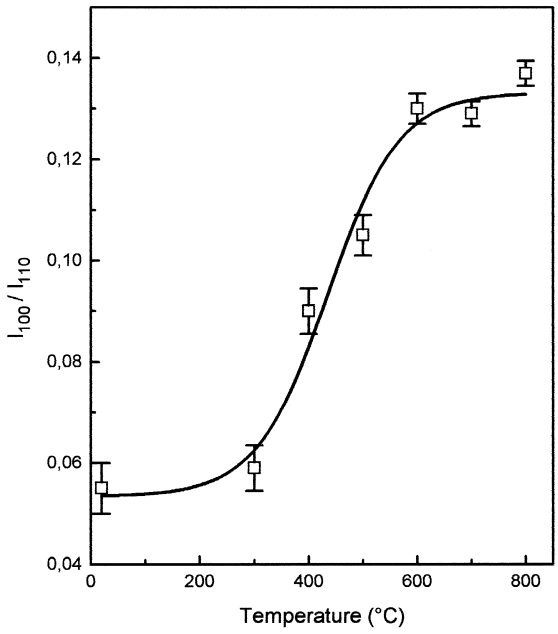

Fig. 6. Evolution vs. annealing temperature of the intensity ratio of the (100) superlattice line to the (110) fundamental line of the B2 structure for the $Al_{50}Ti_{10}Fe_{40}$ alloy.

XRD studies of MA $Al_{50}Ti_{40}Fe_{10}$ and $Al_{50}Ti_{20}Fe_{30}$ powders show that the nanocrystalline structure of these alloys is also preserved after heating up to 500°C.

4. Conclusions

The formation of nanocrystalline single-phase alloys of different structures was observed as a result of mechanical alloying of $Al_{50}Ti_{50-x}Fe_x$ powder mixtures in a high-energy planetary ball mill. The sequence of the structure changes of the MA alloys along the quasibinary section $Al_{50}Ti_{50}$–$Al_{50}Fe_{50}$ can be presented as: hcp(A3)→hcp(C14)→fcc(D8a)→bcc(B2)→bcc(A2). Thus we observed a transition from the more dense hcp structure to the less dense bcc structure when replacing Ti by Fe in the alloys. The nanocrystalline state of the MA alloys is preserved during heating up to 500°C. Annealing at 800°C leads to the formation of the equilibrium phases in agreement with the phase diagram.

Acknowledgements

This work was supported by the program ‘Physics of Constructional and Functional Materials’ of the State Educational Committee of Russia and by grant N 7 TO8D 043 10 of the Warsaw University of Technology.

References

[1] E.M. Shulson, D.R. Barker, Scripta Metall. 17 (1983) 519.
[2] C.C. Koch, Mater. Transact. JIM 36 (1995) 85.
[3] H. Kimura, Sci. Rep. RITU A42 (1996) 245.
[4] A. Inoue, Nanostruct. Mater. 6 (1995) 53.
[5] Y.H. Park, H. Hashimoto, R. Watanabe, Mater. Sci. Forum 88–90 (1992) 59.
[6] L. Shultz, Mater. Sci. Eng. 97 (1988) 15.
[7] B.S. Murty, M.D. Naik, M. Mohan Rao, S. Ranganathan, Mater. Forum 16 (1992) 19.
[8] A.V. Leonov, E. Szewczak, O.E. Gladilina, H. Matyja, V.I. Fadeeva, Mater. Sci. Forum 235–238 (1997) 69.
[9] B. Huang, K.N. Ishihara, P.H. Shingu, Mater. Sci. Eng. A231 (1997) 72.
[10] V.I. Fadeeva, A.V. Leonov, L.N. Khodina, Mater. Sci. Forum 179–181 (1995) 397.
[11] J.Q. Guo, N.S. Kozama, Mater. Sci. Eng. A232 (1997) 177.
[12] M. Palm, G. Inden, N. Thomas, J. Phase Equilibria 16 (1995) 209.
[13] V.I. Fadeeva, A.V. Leonov, E. Szewczak, H. Matyja, Mater. Sci. Eng. A242 (1998) 230.